Journal of Sound and Vibration (1998) **216**(2), 269–279
Article No. sv981669

A WAVE-BASED CONTROLLER DESIGN FOR GENERAL FLEXIBLE STRUCTURES

K. MATSUDA, Y. KANEMITSU AND S. KIJIMOTO

Department of Intelligent Machinery and Systems, *Kyushu University*, 6-10-1 *Hakozaki*, *Fukuoka* 812, *Japan*

(*Received* 11 *October* 1996, *and in final form* 19 *March* 1998)

This paper treats a travelling-wave approach to suppressing vibration of general flexible structures. This approach aims to minimize all of the reflective waves at actuator positions located at the structural boundaries. A variation of the transfer matrix method shows the property that the elastic motion is obtained by superposing the waves travelling in a flexible structure; this transfer matrix method is based on the finite element method for structural analysis. Moreover, the method gives the propagation and scattering relations of the waves in the structure. Since these relations are described by a complex-valued function with respect to Laplace variable, they are transformed into a real-valued form to design a controller by a lot of state–space methods. This transformation is given by diagonalizing the unity transfer matrix into a real-Jordan form. The problem is then formulated as an H_∞ optimization problem to find a compensator minimizing the reflective waves at the actuators. The designed compensator is based only on the scattering relations at the controller positions and on the sensor-input/controller-output relations. A multispan flexible beam is used to verify the validity of the present approach. It is numerically shown that the approach is able to achieve good damping improvement in the closed-loop system.

1. INTRODUCTION

Control of a flexible structure is one of the main themes in control engineering. The dynamical model for the flexible structure is derived from a standing wave in many approaches to solve this problem, whereas travelling-wave approaches are so far limited to the applications to such simple structures as a flexible beam [1, 2]. Now those travelling-wave approaches are briefly described. Elastic waves are generated by a typical force locally applied to the structure, and they might come into a sensor and go out of an actuator. Since the structural responses are represented by superposing the travelling waves, the boundary conditions at an actuator might be written as the relation of the reflective waves with the incident waves and the controller input; this relation is called a scattering relation. The controller input is then set to be in the output-feedback form, which leads to the closed-loop relations between the reflective and incident waves. Moreover, a compensator is selected so as to reduce the effects of the incident waves on the reflective waves in some sense; this reduction is, for example, conducted by setting the elements of the closed-loop scattering matrix at zero. Since those approaches depend on the local structural parts between the sensors and actuators, they can afford to treat such systems that include unknown or unmodelled structural parts. They, however, assume that the system should be described by a partial differential equation. Therefore, it would be difficult to apply the approaches to designing a compensator for complex structures.

In this paper, a travelling-wave approach based on the finite element method is presented. Since the finite element method can be applied to analyzing dynamics of

0022–460X/98/370269 + 11 $30.00/0

complex structures, the approach does not have the afore-mentioned disadvantage of the conventional approaches. The finite element method is now used to formulate the transfer matrix method [3–6]. Moreover, the transfer matrix method is modified to compute the structural responses along the directions in which the waves travel, and gives the scattering and transition relations between the travelling waves; those relations are described by a real-valued function with respect to a Laplace variable in the frequency region. Most of the optimal control methods do not take into account a complex-valued transfer function because a realistic system should be described by a real-valued function. Therefore, a compensator can now be designed by those methods in order to minimize the reflective waves at the actuators. Moreover, this minimization is formulated as an H_∞ optimization problem in this paper. This approach aims to minimize the effects of the incident waves on the reflective waves at the actuators in the sense that the H_∞ norm of the closed-loop scattering matrix is minimum. This can be interpreted as minimizing the worst case H_2 norm of the reflective waves when the incident waves are of finite magnitude, and the design compensator is guaranteed to be a real and causal function. A multispan flexible beam is used as a dynamical model to exemplify the present approach. The open- and closed-loop transfer functions are numerically computed to demonstrate the validity of the designed control system. The results show that good damping improvement is achieved by the present approach.

2. STRUCTURAL DYNAMICS VIA TRAVELLING WAVES

Structural responses can be viewed as a superposition of the waves travelling in a flexible structure. The waves scatter at the structural boundaries and are generated by the external forces acting on the structure. The scattering and generative relations between the waves are essential to designing a compensator and, in this paper, are obtained by a variation of the transfer matrix method [3–6] based on the finite element method. The transfer matrix method is modified to compute the structural responses along the directions in which the waves travel [3]. Further modification is made on the transfer matrix method to use the real-Jordan form of the transfer matrix because a state–space formula is used to design a compensator.

The finite element method is formulated for the ith element of a flexible structure (Figure 1) as follows:

$$\mathbf{Z}_i \begin{bmatrix} \mathbf{q}_i \\ \mathbf{q}_{i+1} \end{bmatrix} = \begin{bmatrix} \mathbf{f}_i \\ -\mathbf{f}_{i+1} \end{bmatrix}, \tag{1}$$

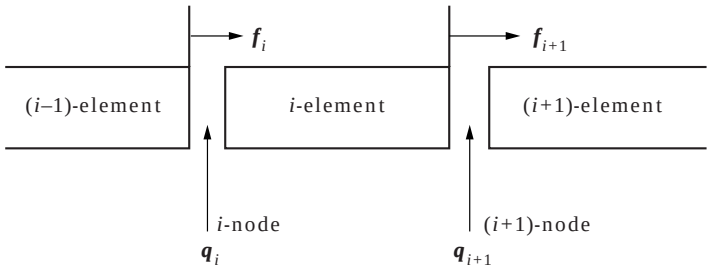

Figure 1. Finite element formulation for structural analysis.

with the impedance matrix

$$\mathbf{Z}_i = -\omega^2\mathbf{M}_i + j\omega\mathbf{C}_i + \mathbf{K}_i = \begin{bmatrix} \mathbf{z}_{11} & \mathbf{z}_{12} \\ \mathbf{z}_{21} & \mathbf{z}_{22} \end{bmatrix}, \tag{2}$$

where $\mathbf{M}_i$, $\mathbf{C}_i$, and $\mathbf{K}_i$ are the unity mass, damping, and stiffness matrices, respectively, for the ith element; the subscript i denotes the element number; the submatrix $\mathbf{z}_{ij}$'s are of the order $p \times p$ with p being a half of the dimension of $\mathbf{Z}_i$; the vectors $\mathbf{q}_i$ and $\mathbf{f}_i$ are the generalized displacement vector and the internal generalized force vector at the ith node. It should be noted that the present system is now Fourier-transformed into the frequency domain.

By making use of some algebraic manipulations, equation (1) is rewritten as

$$\begin{bmatrix} \mathbf{q}_{i+1} \\ \mathbf{f}_{i+1} \end{bmatrix} = \mathbf{T}_i \begin{bmatrix} \mathbf{q}_i \\ \mathbf{f}_i \end{bmatrix} \tag{3}$$

with

$$\mathbf{T}_i = \begin{bmatrix} -\mathbf{z}_{12}^{-1}\mathbf{z}_{11} & \mathbf{z}_{12}^{-1} \\ -\mathbf{z}_{21} + \mathbf{z}_{22}\mathbf{z}_{12}^{-1}\mathbf{z}_{11} & -\mathbf{z}_{22}\mathbf{z}_{12}^{-1} \end{bmatrix}, \tag{4}$$

where $\mathbf{T}_i$ is the transfer matrix, and equations (3) and (4) give the standard transfer matrix formulation using the finite element method. Moreover, we diagonalize the matrix $\mathbf{T}_i$ using the following transformation ($k = i,\ i+1$)

$$\begin{bmatrix} \mathbf{q}_k \\ \mathbf{f}_k \end{bmatrix} = \mathbf{Y}_i \mathbf{w}_k, \tag{5}$$

to obtain the diagonal system

$$\mathbf{w}_{i+1} = \mathbf{L}_i \mathbf{w}_i \tag{6}$$

with

$$\mathbf{L}_i = \mathbf{Y}_i^{-1}\mathbf{T}_i\mathbf{Y}_i = diag[\lambda_1, \lambda_2, \ldots, \lambda_{2p}], \tag{7}$$

where λ_j's and $\mathbf{Y}_i$ are the eigenvalues and eigenvectors of the matrix $\mathbf{T}_i$, respectively. Now we would like to use a property of all of the transfer matrices, that is, there exists a $\lambda_{p+i} = \lambda_i^{-1}$ for every eigenvalue λ_j [6]. This property physically means that each pair of reciprocal eigenvalues is associated with two wave motions propagating with the same form in two opposite directions. By making use of the property, equation (6) may be written as follows:

$$\begin{bmatrix} \mathbf{b}_{i+1} \\ \mathbf{a}_{i+1} \end{bmatrix} = \begin{bmatrix} \mathbf{E}_i & \mathbf{O} \\ \mathbf{O} & \mathbf{E}_i^{-1} \end{bmatrix} \begin{bmatrix} \mathbf{b}_i \\ \mathbf{a}_i \end{bmatrix}, \tag{8}$$

where $\mathbf{E}_i = diag[\lambda_1, \lambda_2, \ldots, \lambda_p]$ and $\mathbf{w}_i = [\mathbf{b}_i^T\ \mathbf{a}_i^T]^T$ is referred to as a wave vector. The eigenvalues of $\mathbf{E}_i$ are arranged such that their eigenvalues are in ascending order; it can be shown that $|\lambda_i| \leqslant 1$ for $1 \leqslant i \leqslant p$ [6]. Furthermore, since those eigenvalues are so arranged, the elements of $\mathbf{a}$ and $\mathbf{b}$ are the complex amplitudes of the waves travelling right and left, respectively. It might be noted that the travelling directions are determined by the causality, that is, the transfer functions from the waves at a downstream point to the waves at an upstream point should be analytic in the right half of the complex plane.

Now a controller is designed using equations (5) and (8). However, it would be difficult to apply such standard state–space formulae as H_∞ control theory to the present system because the matrices $\mathbf{Y}_i$ and $\mathbf{E}_i$ do not satisfy the following condition:

$$\mathbf{H}^*(j\omega) = \mathbf{H}(-j\omega), \tag{9}$$

where $\mathbf{H}(j\omega)$ is a transfer function and the superscript * denotes the complex conjugate. If equation (9) is not satisfied in a system, the system impulse responses take a complex value and the systems with finite dimensions have a state–space realization via complex-valued matrices. Since the state–space formulae cannot be applied to the present system, we transform the matrix $\mathbf{E}_i$ into the real-Jordan form as follows:

$$\tilde{\mathbf{E}}_i = \tilde{\mathbf{Q}}^{-1}\mathbf{E}_i\tilde{\mathbf{Q}} = \mathrm{diag}(\mathbf{e}_1, \mathbf{e}_2, \ldots), \tag{10}$$

with

$$\mathbf{e}_k = \begin{bmatrix} \alpha_k & -\beta_k \\ \beta_k & \alpha_k \end{bmatrix}, \qquad \tilde{\mathbf{Q}} = \mathrm{diag}[\hat{\mathbf{Q}}, \hat{\mathbf{Q}}, \ldots], \quad \text{and} \quad \hat{\mathbf{Q}} = \begin{bmatrix} 1 & j \\ 1 & -j \end{bmatrix}, \tag{11}$$

where $\lambda_k = \alpha_k(j\omega) + j\beta_k(j\omega)$ with α_k and β_k satisfying equation (9) and there exists the eigenvalue $\tilde{\lambda}_k = \alpha_k(j\omega) - j\beta_k(j\omega)$ for every λ_k in the matrix $\mathbf{E}_i$. It might be noted that this real-Jordan form differs from the usual one with λ_k and λ_k^*. Moreover, the transformation yields a new wave vector:

$$\begin{bmatrix} \mathbf{b}_n \\ \mathbf{a}_n \end{bmatrix} = \begin{bmatrix} \tilde{\mathbf{Q}} & \mathbf{O} \\ \mathbf{O} & \tilde{\mathbf{Q}} \end{bmatrix} \begin{bmatrix} \tilde{\mathbf{b}}_n \\ \tilde{\mathbf{a}}_n \end{bmatrix} \equiv \mathbf{Q} \begin{bmatrix} \tilde{\mathbf{b}}_n \\ \tilde{\mathbf{a}}_n \end{bmatrix}, \tag{12}$$

and the state vector also becomes

$$\begin{bmatrix} \mathbf{q}_i \\ \mathbf{f}_i \end{bmatrix} = \mathbf{Y}_i\mathbf{Q}\tilde{\mathbf{w}}_i \equiv \tilde{\mathbf{Y}}_i\tilde{\mathbf{w}}_i. \tag{13}$$

A causal transitional relation of the travelling waves is given by a combination of equations (8) and (15) as

$$\begin{bmatrix} \tilde{\mathbf{b}}_{i+1} \\ \tilde{\mathbf{a}}_i \end{bmatrix} = \begin{bmatrix} \tilde{\mathbf{E}}_i & \mathbf{O} \\ \mathbf{O} & \tilde{\mathbf{E}}_i \end{bmatrix} \begin{bmatrix} \tilde{\mathbf{b}}_i \\ \tilde{\mathbf{a}}_{i+1} \end{bmatrix}. \tag{14}$$

Here, the causality is considered using the simplest example in which the waves propagate through the identical cells labelled from left to right, n through m ($n \leqslant m$), as shown in Figure 2. By making use of equation (14), the wave vectors are related at the two cells as follows:

$$\begin{bmatrix} \tilde{\mathbf{b}}_{m+1} \\ \tilde{\mathbf{a}}_n \end{bmatrix} = \begin{bmatrix} \tilde{\mathbf{E}}^{m-n+1} & \mathbf{O} \\ \mathbf{O} & \tilde{\mathbf{E}}^{m-n+1} \end{bmatrix} \begin{bmatrix} \tilde{\mathbf{b}}_n \\ \tilde{\mathbf{a}}_{m+1} \end{bmatrix}. \tag{15}$$

Figure 2. One-dimensional flexible structure.

Since the eigenvalues of $\tilde{\mathbf{E}}$ are less than unity, the elements of $(\tilde{\mathbf{E}}^{m-n+1})^{-1}$ approach infinity when the total number of elements becomes significantly large. Therefore, the transfer function $\tilde{\mathbf{E}}^{-1}$ cannot be causal when the length of the element is large because it is not analytic in the right-half complex plane. That is why equation (14) gives a causal relation between the travelling waves.

Although the transitional relation was obtained in the previous section, a scattering relation when controller inputs act on a structural boundary is now considered. For simplicity, a one-dimensional flexible structure is considered, as shown in Figure 2. The state and wave vectors are related using equation (13) as follows:

$$\begin{bmatrix} \mathbf{q}_n \\ \mathbf{u} \end{bmatrix} = \begin{bmatrix} \mathbf{M}_{\tilde{b}_n} & \mathbf{M}_{\tilde{a}_n} \\ \mathbf{N}_{\tilde{b}_n} & \mathbf{N}_{\tilde{a}_n} \end{bmatrix} \begin{bmatrix} \tilde{\mathbf{b}}_n \\ \tilde{\mathbf{a}}_n \end{bmatrix}, \tag{16}$$

where $\mathbf{u} = \mathbf{f}_n$ and submatrices, $\mathbf{M}_{\tilde{b}_n}$, $\mathbf{M}_{\tilde{a}_n}$, $\mathbf{N}_{\tilde{b}_n}$ and $\mathbf{N}_{\tilde{a}_n}$, are introduced which are of the order $p \times p$. From the second row of equation (16), one obtains

$$\tilde{\mathbf{b}}_n = \mathbf{S}_n \tilde{\mathbf{a}}_n + \mathbf{V}_n \mathbf{u}, \tag{17}$$

where

$$\mathbf{S}_n = -\mathbf{N}_{\tilde{b}_n}^{-1} \mathbf{N}_{\tilde{a}_n} \quad \text{and} \quad \mathbf{V}_n = \mathbf{N}_{\tilde{b}_n}^{-1}. \tag{18}$$

Equation (17) is called a scatteirng relation, and the structural responses can now be computed through the use of the transitional and scattering relations. For the convenience of the following discussion, the relation between a sensor output and the controller input is considered. Referring again to Figure 2, we let the sensor be at node s ($n \leqslant s$). In the same manner as the scattering relation, the relation between the state and wave vectors is obtained:

$$\begin{bmatrix} \mathbf{y} \\ \mathbf{f}_s \end{bmatrix} = \begin{bmatrix} \mathbf{M}_{\tilde{b}_s} & \mathbf{M}_{\tilde{a}_s} \\ \mathbf{N}_{\tilde{b}_s} & \mathbf{N}_{\tilde{a}_s} \end{bmatrix} \begin{bmatrix} \tilde{\mathbf{b}}_s \\ \tilde{\mathbf{a}}_s \end{bmatrix}, \tag{19}$$

where $\mathbf{y} = \mathbf{q}_s$, and the first row of equation (19) gives

$$\mathbf{y} = \mathbf{M}_{\tilde{b}_s} \tilde{\mathbf{b}}_s + \mathbf{M}_{\tilde{a}_s} \tilde{\mathbf{a}}_s. \tag{20}$$

Some algebraic manipulations using equations (15), (17) and (20) yield

$$\mathbf{y} = \mathbf{J}\tilde{\mathbf{a}}_s + \mathbf{G}\mathbf{u}, \tag{21}$$

where

$$\mathbf{J} = \mathbf{M}_{\tilde{b}_s} \tilde{\mathbf{E}}^{s-n} \mathbf{S}_n \tilde{\mathbf{E}}^{s-n} + \mathbf{M}_{\tilde{a}_s} \quad \text{and} \quad \mathbf{G} = \mathbf{M}_{\tilde{b}_s} \tilde{\mathbf{E}}^{s-n} \mathbf{V}_n. \tag{22}$$

This input–output relation is used to design a compensator in the following section.

3. CONTROLLER DESIGN

Having presented the scattering and transitional relations for the travelling waves in the previous section, we shall now proceed to develop an approach to designing a compensator. This approach is formulated as an H_∞ optimization problem, and readers can refer to the Appendix for some mathematical definitions.

For convenience, our discussion is based on the same example in Figure 2. From equations (15) and (17), the scattering relation might be represented in terms of the incident waves into the sensors to yield

$$\tilde{\mathbf{b}}_n = \tilde{\mathbf{S}}_n \tilde{\mathbf{a}}_s + \mathbf{V}_n \mathbf{u}, \tag{23}$$

where $\tilde{\mathbf{S}}_n = \mathbf{S}_n \tilde{\mathbf{E}}^{s-n}$. We would like to design a compensator which minimizes the reflective waves $\tilde{\mathbf{b}}_n$ in an H_∞ sense. In the H_∞ sense, a compensator is designed to minimize the worst-case amplitude of $\tilde{\mathbf{b}}_n$ in the frequency region. More specifically, the controlled-output vector $\mathbf{v}$ is first selected as

$$\mathbf{v} = \begin{bmatrix} \mathbf{W}_1 \tilde{\mathbf{b}}_n \\ \mathbf{W}_2 \mathbf{u} \end{bmatrix} = \begin{bmatrix} \mathbf{W}_1 \tilde{\mathbf{S}}_n & \mathbf{W}_1 \mathbf{V}_n \\ \mathbf{O} & \mathbf{W}_2 \end{bmatrix} \begin{bmatrix} \tilde{\mathbf{a}}_s \\ \mathbf{u} \end{bmatrix}, \tag{24}$$

where $\mathbf{W}_1$ and $\mathbf{W}_2$ are weighting functions for a design trade-off between $\tilde{\mathbf{b}}_n$ and $\mathbf{u}$ in the frequency region; this trade-off is due to controller limitations. The H_∞ controller design aims to minimize the H_∞ norm of the closed-loop transfer function $\mathbf{D}$ from $\tilde{\mathbf{a}}_s$ to $\mathbf{v}$; the H_∞ norm provides the worst-case $\|\mathbf{v}\|_2$ if $\tilde{\mathbf{a}}_s$ is normalized as follows:

$$\|\mathbf{D}\|_\infty = \sup\left(\|\mathbf{v}\|_2 = \|\mathbf{D}\tilde{\mathbf{a}}_s\|_2 : \|\tilde{\mathbf{a}}_s\|_2 \leqslant 1\right), \tag{25}$$

where $\|\mathbf{v}\|_2^2 = \|\mathbf{W}_1 \tilde{\mathbf{b}}_n\|_2^2 + \|\mathbf{W}_2 \mathbf{u}\|_2^2$. Moreover, the transfer function $\mathbf{D}$ is explicitly written as

$$\mathbf{D} = \begin{bmatrix} \mathbf{W}_1 \mathbf{S}_n' \\ \mathbf{O} \end{bmatrix} + \begin{bmatrix} \mathbf{W}_1 \mathbf{V}_n \\ \mathbf{W}_2 \end{bmatrix} [\mathbf{I} - \mathbf{GP}]^{-1} \mathbf{J}, \tag{26}$$

where the open-loop plant is given by equation (21) and the control input $\mathbf{u}$ is limited to the form $\mathbf{u} = \mathbf{Py}$; $\mathbf{P}$ is a compensator. The problem is now to find the compensator $\mathbf{P}$ to minimize $\|\mathbf{D}\|_\infty$ and solve by a state–space formula [8]. We would like to rewrite the present problem in terms of notation in H_∞ control theory:

$$\begin{bmatrix} \mathbf{v} \\ \mathbf{y} \end{bmatrix} = \begin{bmatrix} \mathbf{W}_1 \mathbf{S}_n' & \mathbf{W}_1 \mathbf{V}_n \\ \mathbf{O} & \mathbf{W}_2 \\ \mathbf{J} & \mathbf{G} \end{bmatrix} \begin{bmatrix} \tilde{\mathbf{a}}_s \\ \mathbf{u} \end{bmatrix}. \tag{27}$$

Note that $\mathbf{J}$ does not satisfy the causality if we use $\tilde{\mathbf{a}}_n$ in place of $\tilde{\mathbf{a}}_s$ in equation (27). The preceding approach has already been applied to the wave-based controller design in a continuous system [7]. Note that the closed-loop stability has not been proved by using this controller design approach.

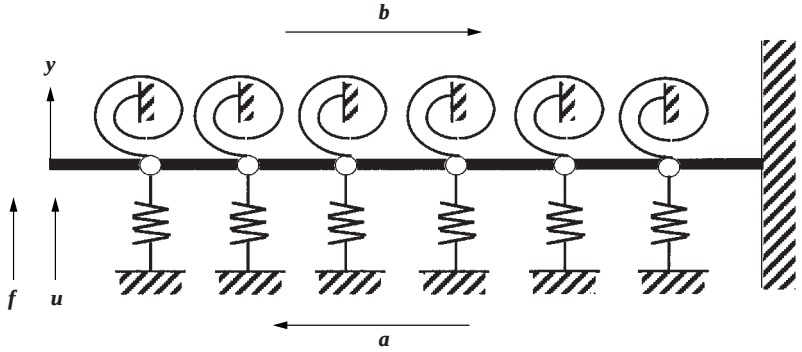

Figure 3. Multispan flexible beam example.

4. MULTISPAN FLEXIBLE BEAM EXAMPLE

A 10-span flexible beam (Figure 3) is used to exemplify the present approach. The clamped–free beam is elastically constrained at nine uniformly spaced interior supports. The validity of the present approach is verified by comparing the open- and closed-loop transfer functions in the frequency region. Moreover, the resultant travelling-wave dynamics and the designed compensator are compared with those of a uniform flexible beam.

In the present example, the cross-sectional state vectors $\mathbf{q}$ and $\mathbf{f}$ are defined as $\mathbf{q} = [\, y \;\; \theta]^T$ and $\mathbf{f} = [m \;\; f\,]^T$, respectively; y is the lateral displacement, θ the slope, m the internal bending moment, and f the internal shear force. Now the unity mass and stiffness matrices for a beam element are used as follows:

$$\mathbf{M} = (\rho A l/420) \begin{bmatrix} 156 & 22l & 54 & -13l \\ 22l & 4l^2 & 13l & -3l^2 \\ 54 & 13l & 156 & -22l \\ -13l & -3l^2 & -22l & 4l^2 \end{bmatrix}, \tag{28}$$

and

$$\mathbf{K} = (2EI(1 + j\varepsilon)/l^3) \begin{bmatrix} 6 & 3l & -6 & 3l \\ 3l & 2l^2 & -3l & l^2 \\ -6 & -3l & 6 & -3l \\ 3l & l^2 & -3l & 2l^2 \end{bmatrix}, \tag{29}$$

where ρA is the mass per unit length, l the length of the unity element, and EI the bending rigidity of the beam; the structural hysteretic damping is used with the imaginary part of the rigidity, $\varepsilon = 1{\cdot}0 \times 10^{-7}$; the unity damping matrix $\mathbf{C}$ is the null matrix; all of the physical parameters are set to be those of reference [4], that is, the beam length is 4·0 m, $EI = 2{\cdot}0 \times 10^6$ Nm^2, and $\rho A = 8{\cdot}9 \times 10^1$ kg/m; the beam is divided into ten elements with equal length. Moreover, the beam is elastically constrained at each support, and the transfer matrix associated with the support is written as

$$\mathbf{F} = \begin{bmatrix} 1 & 0 & 0 & 0 \\ 0 & 1 & 0 & 0 \\ 0 & -k_2 & 1 & 0 \\ -k_1 & 0 & 0 & 1 \end{bmatrix}, \tag{30}$$

where k_1 and k_2 are the deflectional and rotational spring-constants of an elastic support, respectively; $k_1 = 1{\cdot}0 \times 10^5$ N/m and $k_2 = 1{\cdot}0 \times 10^5$ N/rad.

Equations (2), (4), (28) and (29) are combined to give the transfer matrix $\mathbf{T}$ for a beam element; the matrix $\mathbf{T}$ is transformed into the real Jordan form $\mathbf{L}$ to give

$$\begin{bmatrix} \tilde{\mathbf{b}}_{i+1} \\ \tilde{\mathbf{a}}_{i+1} \end{bmatrix} = \mathbf{L} \begin{bmatrix} \tilde{\mathbf{b}}_i \\ \tilde{\mathbf{a}}_i \end{bmatrix}, \tag{31}$$

where $\mathbf{L} = \tilde{\mathbf{Y}}^{-1}\mathbf{T}\tilde{\mathbf{Y}}$. Figure 4 shows frequency responses of the eigenvalues of the transfer matrix $\mathbf{T}$; only the first two eigenvalues are shown in this figure, and they are not more than unity in magnitude, as shown in the previous section. Moreover, the same

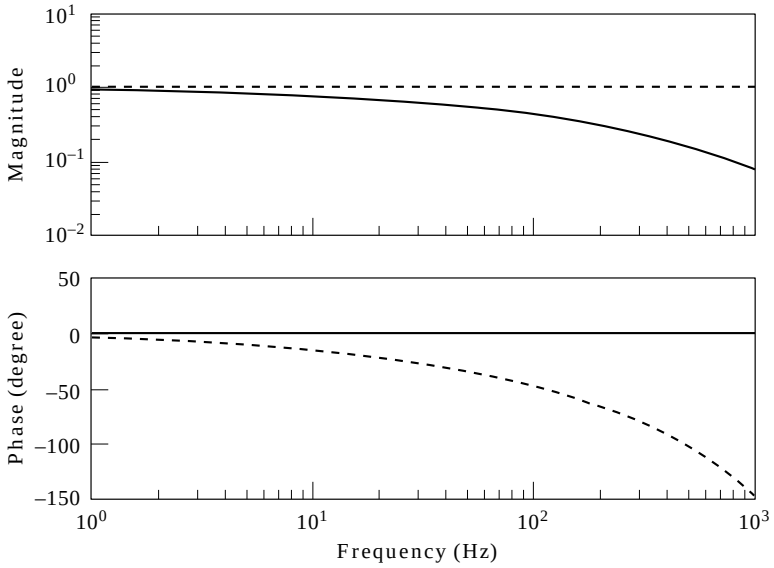

Figure 4. The transfer functions of the eigenvalues of the transfer matrix (λ_1: solid, λ_2: dashed).

transformation is applied to the matrix **F** to yield the travelling-wave dynamics at each support:

$$\begin{bmatrix} \tilde{\mathbf{b}}_{j+1} \\ \tilde{\mathbf{a}}_{j+1} \end{bmatrix} = \mathbf{R} \begin{bmatrix} \tilde{\mathbf{b}}_j \\ \tilde{\mathbf{a}}_j \end{bmatrix}, \tag{32}$$

where $\mathbf{R} = \tilde{\mathbf{Y}}^{-1}\mathbf{F}\tilde{\mathbf{Y}}$. It might be noted that the travelling waves could be reflected and transmitted at each support because the matrix **R** does not take a diagonal form.

Now the scattering relation is obtained at the left end; this end is modelled as a beam element. Since a force actuator is now located at this end, the scattering relation is given by equations (17) and (18) as

$$\tilde{\mathbf{b}}_0 = \mathbf{S}_0\tilde{\mathbf{a}}_0 + \mathbf{V}_0 u \tag{33}$$

where

$$\mathbf{S}_0 = -\mathbf{N}_{\tilde{b}_0}^{-1}\mathbf{N}_{\tilde{a}_0} \quad \text{and} \quad \mathbf{V}_0 = \mathbf{N}_{\tilde{b}_0}^{-1}[0 \quad 1]^T. \tag{34}$$

Since a displacement sensor is collocated with a force sensor at the free end, the input–output relation is obtained using equations (21) and (22):

$$\mathbf{y} = \mathbf{J}\tilde{\mathbf{a}}_s + \mathbf{G}\mathbf{u}, \tag{35}$$

where

$$\mathbf{J} = [1 \quad 0](\mathbf{M}_{\tilde{b}_0}\mathbf{S}_0 + \mathbf{M}_{\tilde{a}_0}) \quad \text{and} \quad \mathbf{G} = [1 \quad 0]\mathbf{M}_{\tilde{b}_0}\mathbf{V}_0. \tag{36}$$

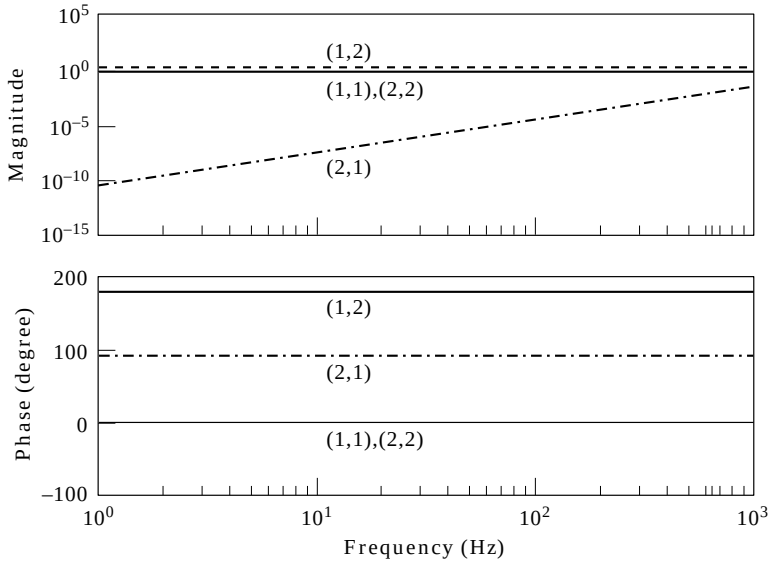

Figure 5. The transfer functions of the elements of the scattering matrix.

In fact, these two relations are numerically obtained as frequency response data (Figure 5), and the frequency responses are fitted with a curve to yield a model of equations (33) and (35).

$$\tilde{\mathbf{b}}_0 = \begin{bmatrix} 1{\cdot}0 & 2{\cdot}0 \\ 10^{-13}s^3 & -1{\cdot}0 \end{bmatrix} \tilde{\mathbf{a}}_0 + \begin{bmatrix} 5{\cdot}0 \times 10^{-4} s^{-3/2} \\ -4{\cdot}0 \times 10^{-17} s^{3/2} \end{bmatrix} u \tag{37}$$

and

$$y = 1{\cdot}0 \times 10^{-3} s^{-3/2} u + [0{\cdot}4 \quad 0{\cdot}4]\tilde{\mathbf{a}}_0, \tag{38}$$

where the deviations are significantly small from the frequency response data. The multispan beam is modelled as a beam element at the left end. If the two relations are now compared with those using a uniform flexible beam, it is found that equation (37) contains significantly smaller terms in place of zeros; the uniform flexible beam is modelled as a Euler–Bernoulli beam. Those small terms are now set to zero because they are smaller than the other terms by about 40 dB at 10^3 Hz. The first eight natural frequencies are below this frequency, whereas the beam now contains ten elements. Therefore, the model is less reliable over the frequency region above 10^3 Hz. An optimal compensator is obtained analytically in the same manner as the continuous system [7] as follows:

$$P = -2{\cdot}3 \times 10^3 \, s^{3/2}. \tag{39}$$

Figure 6 shows the open- and closed-loop transfer function from a disturbance force input to the displacement sensor at the free end of the beam. It is shown that good damping improvement has been achieved by the designed controller. Note that the first natural frequency of the present system deviates by 16% from that of a uniform flexible beam.

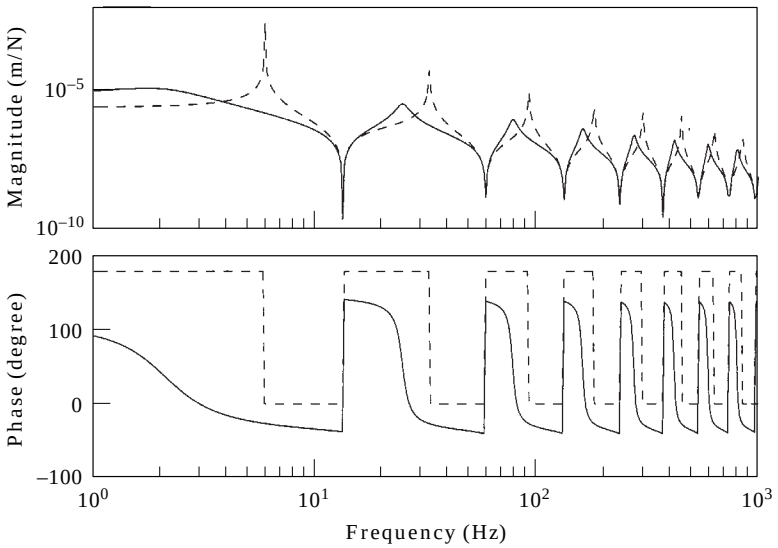

Figure 6. The open- (dashed) and closed-loop (solid) transfer functions from f to y.

5. CONCLUSIONS

A variation of the transfer matrix method is used to show that elastic motion is a superposition of the waves travelling in a flexible structure. This transfer function method is based on the finite element method and diagonalizes the unity transfer matrix into the real-Jordan form. Moreover, the transitional and scattering relations between the waves are obtained through the use of this method; these relations are used to design a controller. The problem is formulated as an H_∞ optimization problem to find a compensator minimizing the reflective waves at the actuators subject to the constraints on the controller input. A multispan flexible beam is used to exemplify the present approach. The clamped–free beam is elastically constrained at uniformly spaced interior supports. The open- and closed-loop transfer function from a disturbance force input is compared to the displacement sensor at the free end of the beam. The result shows that good damping improvement has been achieved by the designed controller.

REFERENCES

1. D. R. Vaughan 1968 *Journal of Basic Engineering* **June**, 157–166. Application of distributed parameter concepts to dynamical analysis and control of bending vibrations.
2. A. H. von Flotow 1986 *American Institute of Aeronautics and Astronautics Journal of Guidance, Control, and Dynamics* **9**, 462–468. Traveling wave control for large spacecraft structures.
3. Y. Yong and Y. K. Lin 1990 *American Institute of Aeronautics and Astronautics Journal* **28**, 1250–1258. Dynamics of complex truss-type space structures.
4. J.-J. Yu and A. Craggs 1995 *Journal of Sound and Vibration* **187**, 169–175. Transfer matrix method for finite element models of a chain-like structure under harmonic excitations.
5. J. Signorelli and A. H. von Flotow 1988 *Journal of Sound and Vibration* **187**, 127–144. Wave propagation, power flow, and resonance in a truss beam.
6. Y. K. Lin and T. J. McDaniel 1969 *The American Society of Mechanical Engineers Journal of Engineering for Industry* **91**, 1133–1141. Dynamics of beam-type periodic structures.
7. K. Matsuda and H. Fujii 1993 *American Institute of Aeronautics and Astronautics Journal of Guidance, Control, and Dynamics* **16**, 1146–1153. H_∞ optimized wave-absorbing control: analytical and experimental results.

8. K. Glover, D. J. N. Limebeer, J. C. Doyle, E. M. Kasenally and M. G. Safonov 1991 *SIAM Journal of Control and Optimization* **29**, 283–324. A characterization of all solutions to the four block general distance problem.

APPENDIX

We define $\|\mathbf{A}\|_\infty$ (the H_∞-norm of a matrix $\mathbf{A}$) as follows:

$$\|\mathbf{A}\|_\infty = \max_\omega \bar{\sigma}(\mathbf{A}(j\omega)), \tag{A1}$$

where $\bar{\sigma}$ denotes the largest singular value, and $\|\mathbf{A}\|_2$ (the H_2-norm of $\mathbf{A}$) is given by

$$\|\mathbf{A}\|_2 = \left\{(1/2\pi)\int_{-\infty}^{\infty} trace[\mathbf{A}^H(j\omega)\mathbf{A}(j\omega)]\,\mathrm{d}\omega\right\}^{1/2}, \tag{A2}$$

where the superscript H denotes the Hermite conjugate transpose. Moreover, we show the relation between the H_∞- and H_2-norms:

$$\|\mathbf{A}\|_2 = \sup(\|\mathbf{Ax}\|_2 : \|\mathbf{x}\|_2 \leqslant 1). \tag{A3}$$